Resolvent Analysis of Shock Buffet on Infinite Wings

Wei He* and Sebastian Timme†
University of Liverpool, Liverpool, L69 3GH, United Kingdom

Resolvent analysis to identify the unsteady aerodynamic response to harmonic forcing (interpreted as higher-order non-linear terms in the governing equations or external) is presented for three-dimensional infinite straight and swept wings without assumptions on spatial spanwise homogeneity (so-called triglobal). This work continues the recent triglobal modal stability analysis by He and Timme [1] and expands upon the elucidation of shock-buffet flow physics presented earlier in Sartor et al. [2] for two-dimensional aerofoil flow. The flow conditions are a freestream Mach number of 0.73 with a reference chord Reynolds number of 3.2×10^6 and angles of attack describing pre- and post-onset shock-buffet conditions. The infinite wing is modelled as a rectangular geometry with a chosen aspect ratio of 3 and spanwise periodic boundary condition imposed. The base flow is solved in the framework of steady Reynolds-averaged Navier–Stokes equations with a closure using the negative Spalart–Allmaras turbulence model and assumed to be spanwise parallel both for the infinite straight and swept wings. The novel algorithm, following the work by Gómez et al. [3], without the need to evaluate the resolvent operator explicitly enables the efficient computation of optimal forcing and response modes together with the amplification gain at arbitrary frequencies. At the flow conditions investigated, a high amplification is found at a low Strouhal number of $St \approx 0.06$ to 0.07 coinciding with the well-known two-dimensional aerofoil shock-buffet mode, both on straight and swept wings. Spanwise-periodic resolvent modes are observed at $St < 0.03$ for the straight wing and $St = 0.1$ to 1 for the swept wing. These results for the spanwise-periodic modes are consistent with recent global stability studies on infinite wings. For yet higher Strouhal numbers, specifically $St = 1$ to 5, another mode, resembling a Kelvin–Helmholtz shear-layer instability, is observed. The results suggest, particularly for the subcritical flow, that resolvent analysis is a powerful tool to detect modes of an imminent instability early when global stability analysis would fail.

Nomenclature

C_L	=	lift coefficient
C_p	=	pressure coefficient
c	=	chord length
J	=	Jacobian matrix
M	=	Mach number
R	=	Resolvent operator
Re	=	Reynolds number
St	=	Strouhal number $St = \omega/(2\pi)$
U_{ref}	=	reference velocity perpendicular to leading edge
U_∞	=	freestream velocity
α	=	angle of attack (°)
λ	=	eigenvalue of modal analysis ($\lambda = \sigma + i\omega$)
ω	=	frequency of eigenvalue
σ	=	growth rate of eigenvalue
Λ	=	sweep angle (°)

*Research Associate, School of Engineering, wei.he@liverpool.ac.uk.
†Senior Lecturer, School of Engineering, sebastian.timme@liverpool.ac.uk. Member AIAA.

I. Introduction

Shock buffet brings a challenge to the wing design of modern large transport-type aircraft when flying in the transonic regime. Shock buffet will exert additional low-frequency aerodynamic loads on the wing affecting the flight performance and potentially causing damage to the structure. Jacquin et al. [4] documented a stable shock in the transonic flow ($M = 0.73$, $Re \approx 3\times10^6$) of a low aspect ratio (approximately 3) wing at an angle of attack $\alpha < 3°$. With increasing angle of attack, the shock becomes unstable leading to a strong oscillation of the shock-wave/turbulent boundary layer interaction, referred to as 'shock buffet', at about $\alpha = 3.5°$. After shock buffet initiates, a three-dimensional flow pattern is formed in the separation zone behind the unsteady shock. It is similar to the so-called *stall cells* observed in the flow of severe separation from low to high Reynolds numbers [5–9]. Numerical simulations on different aerofoils at high Reynolds numbers featuring shock oscillations showed that the flow can be solved when using the unsteady Reynolds-averaged Navier–Stokes (RANS) equations and an appropriate turbulence model [10, 11]. The prediction of shock-buffet onset at flight conditions is nevertheless expensive regardless whether flight test, wind tunnel experiment or time-stepping unsteady simulation is used, and a modal approach based on the linearised governing equations is a powerful alternative method [12–14]. As such the transonic shock-buffet stability has been well documented numerically in the two-dimensional flow using the NACA 0012 aerofoil [12] and more recently using other supercritical aerofoil geometries [2, 15]. Three-dimensional shock buffet has also been studied on infinite wings and practical finite-wing aircraft [9, 13–16]. Recently, fully three-dimensional infinite-wing flow without limitations on the spanwise flow development (by removing the assumption of spanwise homogeneity) has been investigated by He and Timme [1]. Besides the nominal two-dimensional aerofoil mode often reported in literature, spanwise-periodic cellular modes are identified on straight and swept wings of different aspect ratios.

Linearised aerodynamics stability analysis requires the limiting assumption of small amplitudes and hence non-linear effects are omitted. However, on the one hand, it has been demonstrated that non-linear effects based on the mean flow can be analysed to obtain the correct perturbation frequency [17, 18]. On the other hand, the intrinsic non-linear effects of the fluid or an external forcing can lead to high-amplitude responses [19], which can be systematically studied through the resolvent analysis. Resolvent analysis has been successfully applied in various studies, such as in aerodynamic force reconstruction [3] or turbulent-aerofoil flow control [20]. Sartor et al. [2] considered two-dimensional resolvent analysis for the OAT15A aerofoil at $M = 0.73$ and $Re = 3.2\times10^6$ for the angle of attack range $\alpha = 2.5°$ to $7°$ (corresponding to the aerofoil and flow conditions investigated herein). They identified the most amplified gain at Strouhal number $St \approx 0.07$ for post-onset shock-buffet flow at $\alpha = 3.5°$, which corresponds to the therein also reported globally unstable aerofoil mode. At higher frequencies, external forcing resulted in a Kelvin–Helmholtz-type mode in the shear layer behind the shock. Besides the research mentioned above, to the authors' knowledge, there are no resolvent studies published for three-dimensional infinite-wing shock-buffet flow. In this spirit, recent advances in numerical algorithms allow the investigation of fully three-dimensional problems without assumptions on the base flow.

In this paper, resolvent analysis is performed for infinite straight and swept wing flow, mainly focusing on the condition near the onset of self-sustained shock-buffet unsteadiness, including globally stable and unstable flow. The theory behind resolvent analysis is briefly introduced in Sec. II and the numerical setup is detailed in Sec. III. Section IV presents results of the resolvent analysis of pre- and post-onset shock-buffet flow on straight and swept wings.

II. Theory

Resolvent analysis aims to investigate the optimal response to a harmonic non-linear and/or external forcing to a flow system [21]. Define the state vector $\mathbf{q}$ containing the conservative variables, specifically $\mathbf{q} = (\rho, \rho\mathbf{u}, \rho E, \rho\tilde{\nu})^{\mathrm{T}}$, where ρ is the density, $\rho\mathbf{u}$ are the three momentum components, ρE is the total energy and $\rho\tilde{\nu}$ relates to the turbulence model. For a given compressible flow field, $\mathbf{q}$ can be decomposed as $\mathbf{q} = \bar{\mathbf{q}} + \tilde{\mathbf{q}}$, where $\bar{\mathbf{q}}$ is the non-linear steady base flow and $\tilde{\mathbf{q}}$ is the perturbation, respectively. Then, the semi-discretised RANS equations coupled with a suitable turbulence model can be linearised as

$$\frac{\mathrm{d}\tilde{\mathbf{q}}}{\mathrm{d}t} = J\tilde{\mathbf{q}} + \tilde{\mathbf{f}}, \tag{1}$$

where J is the linear operator (i.e. the Jacobian matrix) and $\tilde{\mathbf{f}}$ represents either nonlinear terms of the governing equations or an external forcing. Suppose the external forcing and resulting perturbation are harmonic, then

$$\tilde{\mathbf{q}} = \hat{\mathbf{q}}e^{i\omega t}, \quad \tilde{\mathbf{f}} = \hat{\mathbf{f}}e^{i\omega t} \tag{2}$$

where $\hat{\mathbf{q}}$ and $\hat{\mathbf{f}}$ describe complex spatial amplitudes and ω is the forcing frequency. Equation (1) can be written as

$$\hat{\mathbf{q}} = -R\hat{\mathbf{f}}, \tag{3}$$

where $R = (J - i\omega I)^{-1}$ is the resolvent operator and I is the identity matrix. For a given forcing with angular frequency ω, its optimal response is defined by the maximum amplification or gain

$$G = \max \frac{< \hat{\mathbf{q}},\ \hat{\mathbf{q}} >_Q}{< \hat{\mathbf{f}},\ \hat{\mathbf{f}} >_Q} = \max \frac{\hat{\mathbf{q}}^* Q \hat{\mathbf{q}}}{\hat{\mathbf{f}}^* Q \hat{\mathbf{f}}} = \max \frac{\hat{\mathbf{f}}^* R^* Q R \hat{\mathbf{f}}}{\hat{\mathbf{f}}^* Q \hat{\mathbf{f}}}, \tag{4}$$

where $< \mathbf{u},\ \mathbf{v} >_Q = \mathbf{u}^* Q \mathbf{v}$ defines an inner product on arbitrary vectors $\mathbf{u}$ and $\mathbf{v}$, with $\mathbf{u}^*$ as the Hermitian transpose of $\mathbf{u}$, and Q is a chosen positive definite diagonal matrix containing the discrete cell volumes herein. Other inner products have been discussed in the literature [20, 22, 23]. The solution of the resolvent problem can be achieved by solving the singular value decomposition of R [3]. The left and right singular vectors then describe the optimal response and forcing modes, respectively, while the singular values σ_j describe the optimal gain. Alternatively, the largest eigenmodes of R^*R and RR^* give the same information, where R^* is the adjoint resolvent operator defined through the inner product, specifically, $< \mathbf{u}, R\mathbf{v} >_Q = < R^*\mathbf{u}, \mathbf{v} >_Q$. Importantly, with an appropriate iterative scheme, forming the resolvent operator explicitly is not required to compute the dominant solution provided $\sigma_1 > \sigma_j$ for $j = 2, ..., n$. Here, n denotes the dimension of the discretised fluid system.

The linear eigenvalue problem

$$(J - \lambda I)\, \hat{\mathbf{q}} = 0 \tag{5}$$

is found, when the right-hand side forcing term of eqn. (1) is eliminated, where $\lambda = \sigma + i\omega$ is the complex eigenvalue with σ as the growth rate.

III. Numerical Setup

The base flow is obtained by solving the steady RANS equations using the DLR–TAU solver, which is a second-order finite-volume code capable of dealing with complex geometries [24], widely used in the European aerospace industry and academia. For modelling the Reynolds stresses we make use of the Boussinesq approximation with eddy viscosity provided through the negative version of the Spalart–Allmaras (S–A) turbulence model [25]. The inviscid fluxes of the mean flow equations are discretised using a central scheme with matrix artificial dissipation, whereas a first-order Roe scheme is used for those of the turbulence model. Gradients of flow variables are computed using the Green–Gauss approach. As time-stepper for the steady-state solutions, we use an explicit Runge–Kutta scheme with local time-stepping and geometric multigrid (normally on 3 grid levels) for convergence acceleration. For time-marching unsteady simulations, we use standard second-order dual-time stepping, with the steady-state time-stepper employed on the subiteration level of each physical time step.

A triglobal linearised aerodynamics tool, comprising the capability of global stability analysis and resolvent analysis, has been implemented in the TAU code previously and its ability for stability studies demonstrated in [14, 16]. The numerical approach follows a first-discretise-then-linearise matrix-forming philosophy, with a hand-differentiated Jacobian matrix, using an iterative inner-outer solution scheme. The steady-state RANS solution fully coupled with the turbulence model is used as base flow, around which the linearised system is formed. For stability analysis, we use the implicity restarted Arnoldi method (provided by the ARPACK library) to approximate a few but relevant eigenmodes in the outer iteration [26–28]. A preconditioned sparse iterative Krylov subspace solver is applied for the repeated solution of arising large linear systems of equations. For the inner-outer iterative scheme of the resolvent analysis, we adopted and adapted the algorithm presented in [3]. The established numerical strategy combined with an industrial computational fluid dynamics solver means that even practical non-canonical test cases at high Reynolds number flow condition can be investigated, provided a decoupling of scales between coherent large scale fluctuations, dominating the flow dynamics, and the small scales of turbulence can be assumed.

Infinite-wing flow is investigated herein. A three-dimensional (3D) infinite straight wing geometry is generated by extruding a two-dimensional (2D) OAT15A aerofoil in spanwise direction with 20 uniformly-spaced grid layers per unit span. This aerofoil is well documented in previous studies [2, 4, 13]. Our focal infinite wing, with approximately 2.1×10^6 points in total and 35,000 points for the 2D mesh, has an actual aspect ratio of $\mathit{AR} = 3$ (see fig. 1*a*), as it describes the smallest span to allow a pair of stall cells to develop, cf. the discussion in [1]. Spanwise periodic boundary condition is imposed in translation and viscous wall and far field are defined on the wing and the outer boundary, respectively. Even though not shown, additional wings of different aspect ratios were scrutinised giving consistent results to those analysed herein. A more detailed grid convergence and geometry study can be found in [1].

Swept wings delay the formation of shock waves by increasing the critical Mach number normal to the leading edge compared to straight wings. In order to simplify the swept-wing simulation setup, a sideslip velocity component is

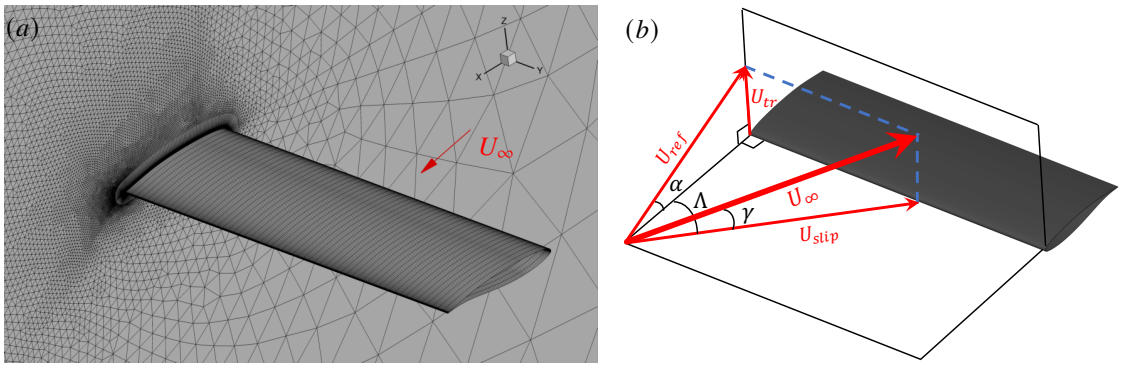

Fig. 1 Mesh around the wing with $\mathit{AR} = 3$ (a) and swept flow definition (b).

added and the flow conditions normal to the leading edge of the wing are enforced to be the same as for the straight wing. Figure 1b shows the definition of a flow past the wing with a non-zero sweep angle Λ. For an expository description of the applied transformations, we have

$$\begin{aligned} U_\infty &= \frac{U_{\text{ref}}}{\cos\Lambda}\sqrt{1-\sin^2\alpha\,\sin^2\Lambda} \\ Re_\infty &= \frac{Re_{\text{ref}}}{\cos\Lambda}\sqrt{1-\sin^2\alpha\,\sin^2\Lambda} \\ \gamma &= \operatorname{atan}(\tan\alpha\,\cos\Lambda) \end{aligned} \tag{6}$$

where the parameters α, U_{ref} and Re_{ref} are the components of angle of attack, reference velocity and Reynolds number perpendicular to the leading edge of the wing, respectively. These are visualised in the figure.

IV. Results

A. Base Flow

Preparing a steady transonic flow featuring shock buffet on a straight or swept wing for subsequent stability and resolvent analysis is of pivotal importance. The flow condition is consistently defined in the plane perpendicular to the leading edge. At a Mach number of $M = 0.73$ and a chord Reynolds number of $Re = 3.2 \times 10^6$, we investigate two angles of attack α near the onset of self-sustained shock-buffet unsteadiness, specifically the subcritical $\alpha = 3.0°$ and the supercritical $\alpha = 3.5°$. The surface pressure coefficient C_p on both the straight and swept wings (with sweep angle $\Lambda = 20°$) of the steady RANS solution is shown in fig. 2. The base flow is naturally parallel in spanwise direction for the straight wing without enforcing spanwise homogeneity. A strong shock is observed around the mid-chord location, and a thin separation bubble forms at the foot of the shock and extends to trailing edge, as shown in the amplified subplot in fig. 2a. The result is obtained at a density-residual norm of about 10^{-8}, which is well below typical convergence levels used in industry. The flow will generate stall cells, even for the straight wing, when steady-state iterations are continued to machine precision [1]. According to eqn. (6), freestream values are adjusted to form a flow over a wing with $\Lambda = 20°$ sweep angle. Since the flow conditions normal to leading edge are enforced to be equal (independent of sweep angle), the flow in the $xz-$plane shows negligible difference to the straight-wing flow. The swept-wing flow in spanwise direction is also parallel (see fig. 2b).

The pressure coefficient at the mid-span of the two wings compared to the experimental results [4] is presented in fig. 3. The difference between experimental and numerical angle of attack is well documented in the literature. In our simulations, the so-called compressibility correction to the S–A turbulence model [29], first used in a NACA 0012 aerofoil transonic flow stability study [12], is not activated. This term shows a strong influence on the results, yielding a reduction of onset angle of approximately 0.3° to 0.5° [15]. The experimental results suggest a steady flow for $\alpha = 3.0°$ due to the sharp shock, which becomes smeared for $\alpha = 3.5°$ suggesting shock motion of about 20% chord extent. Consequently, our simulation results at $\alpha = 3.5°$ agree more closely to the experiment at $\alpha = 3.0°$.

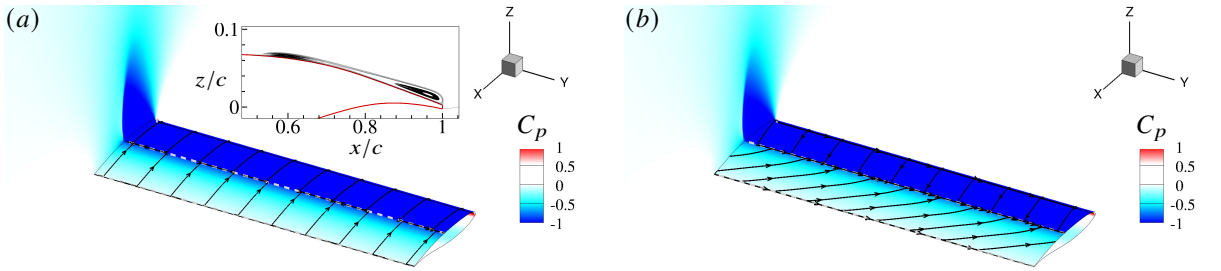

Fig. 2 Surface pressure coefficient C_p on (a) straight and (b) swept (with sweep angle $\Lambda = 20°$) wings at $\alpha = 3.5°$. Surface skin-friction lines and zero skin-friction line are highlighted by black and grey dashed lines, respectively. The separation bubble is visualised in (a). The periodic boundary plane at $y_{\min} = 0$ is shown.

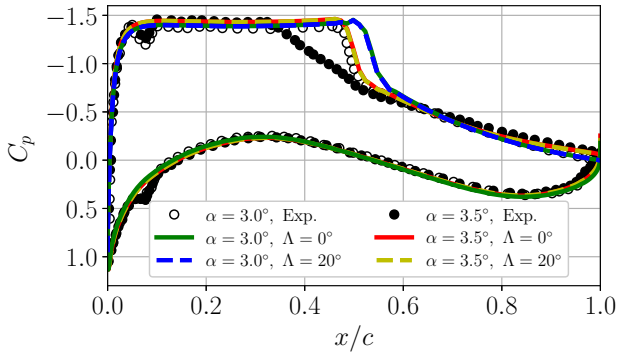

Fig. 3 Surface pressure coefficient C_p along mid-span, compared with experiments from [4]. Note that C_p for swept wing has been normalised by reference values normal to leading edge rather than freestream values.

B. Overview of Previous Global Stability Results

In previous studies, see [1] for a detailed discussion, besides an aerofoil shock-buffet mode with angular frequency of approximately $\omega = 0.44$ (corresponding to a Strouhal number of $St \approx 0.07$), several monotone (zero frequency) unstable modes with spanwise-periodic cellular patterns were identified in supercritical spanwise-parallel base flow at $\alpha = 3.5°$ on the straight wing (see fig. 4a). These modes have the effect of distorting the shock front, when non-linear saturation kicks in, and discretise the continuous band of modes observed in biglobal studies [9, 13, 15]. For the straight wing, the most amplified spanwise-periodic mode is the one with wavelength $1c$ (i.e. three cells for the $\mathcal{AR} = 3$ wing). The frequency of those spanwise modes grows as the sweep angle increases, e.g. to $\Lambda = 20°$, and eventually exceeds the aerofoil-mode frequency (see fig. 4b). As shown in fig. 4, no unstable global mode is found at angle of attack $\alpha = 3.0°$, neither for straight nor swept wing, with the chosen numerical setup.

How this infinite parallel flow itself responds to the external forcing, e.g. noise or active flow control, needs to be scrutinised. It is possible to investigate this point through the resolvent approach.

C. Resolvent Analysis

The resolvent results are presented in figs. 5 through 8. Figures 5 and 6 present the optimal gain G due to harmonic forcing at a given Strouhal number, at both pre- and post-onset shock-buffet conditions, for the infinite straight and swept wings, respectively. The magnitude of the unsteady lift, $|\widehat{C}_L|$, integrated from the pressure distribution of the response mode is shown therein as well. The corresponding spatial structures of forcing and response resolvent modes are shown in figs. 7 and 8. For a given forcing frequency, the inner-outer solution scheme typically requires between 10 and 30 outer iterations, converging the norm of the forcing-vector update by four orders of magnitude. On each outer iteration, the inner iterations of the forward and adjoint solutions are converged seven orders of magnitude in about 600 iterations each. Note, in contrast to the work in e.g. [16, 30], our forcing is within the fluid system rather than through the domain boundary (such as the deflection of a control surface or a moving wing).

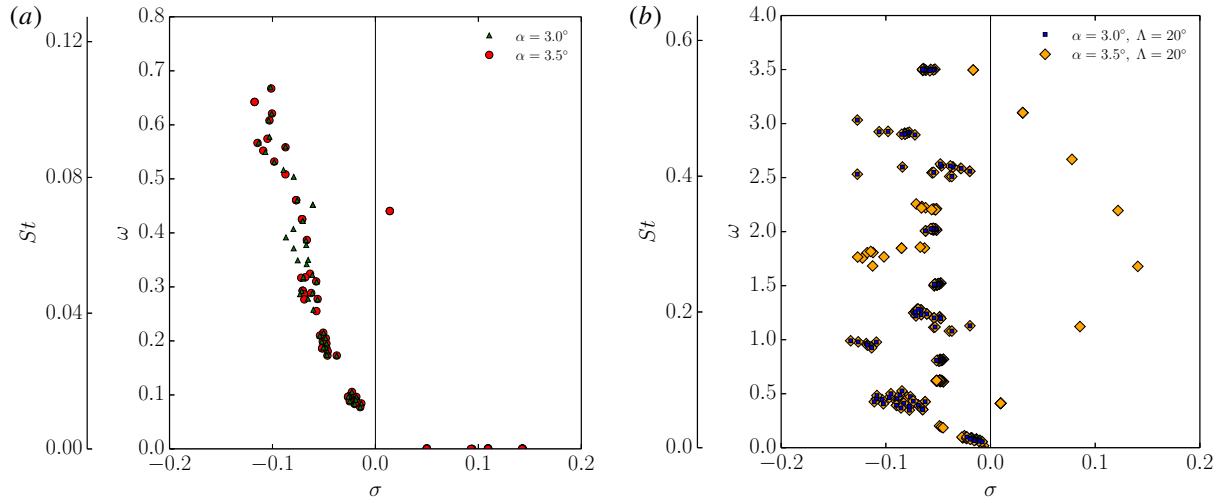

Fig. 4 Eigenspectra for (*a*) straight and (*b*) swept wings at two angles of attack around onset of shock buffet.

The optimal gain in figs. 5*a* and 6*a* suggests that there are three distinct Strouhal-number regions for the straight and swept wings at pre- and post-onset shock-buffet conditions. In fig. 5*a*, for the straight-wing resolvent analysis in supercritical flow at $\alpha = 3.5°$, the first region is at very low Strouhal numbers $St < 0.03$, followed by a distinct peak at $St \approx 0.06$ and a third region in the range $St \approx 1$ to 5. The forcing at very low frequencies results in a strong resonance with the monotone modes observed in the stability analysis. It can be demonstrated that the resolvent operator is very close to the inverse of the Jacobian matrix because the term $i\omega I$ approaches zero. In the pre-onset condition of shock buffet at $\alpha = 3.0°$, the gain is nearly constant at these low frequencies and much lower than that at the higher angle of attack, which is consistent with the global-stability findings (see fig. 4*a*), where no unstable monotone modes are observed. In the range $St \approx 1$ to 5, the optimal gain has a similar trend for both angles of attack. Importantly, a high peak of the optimal gain can be observed at $St \approx 0.07$, corresponding to the aerofoil shock-buffet mode excited through an appropriate forcing, for both angles of attack. Similar behaviour is observed for the swept-wing case in fig. 6a, albeit regions 1 and 2 (for the straight wing) swapping positions for the swept wing. The key difference is in the Strouhal-number region $St \approx 0.1$ to 1.0, which now shows higher gains, while the low-frequency excess gains seem to vanish. For instance for supercritical angle of attack $\alpha = 3.5°$, a highly concentrated peak is observed at $St \approx 0.5$ to 0.6, which agrees with the spanwise-periodic modes closest to the imaginary axis in fig. 4*b*. The resolvent discussion reveals that, on the one hand, the dominant modes from the global stability analysis are identified, even in subcritical flow, and, on the other hand, an additional higher-frequency mode is present, similar to previous aerofoil studies [2]. The impact of the inherent non-normality in the governing equations, in contrast to the trivial distance between eigenvalue and forcing frequency, $|\lambda - i\omega|$, particularly for the subcritical flow, requires a more thorough investigation [22].

Representative spatial structures within these three distinct regions are presented in figs. 7 and 8, for straight and swept wing, respectively. While fig. 7 is for the supercritical $\alpha = 3.5°$, we chose to visualise the subcritical results on the swept wing in fig. 8. We observed little change in the underlying modal structures when crossing the critical condition of global instability onset. Together with the gain, spatial structures can be interpreted as the energy distribution of the optimal forcing and its corresponding response modes in the flow system. Take the resolvent results at a frequency close to the origin ($St \approx 0.001$), the forcing and response modes (visualised by the real part of the energy fluctuation $\mathcal{R}\{\widehat{\rho E}\}$) are shown in fig. 7*a* and *b*. The five-cell spanwise-periodic response mode has a structure similar to the monotone mode closest to the origin in the eigenspectrum in fig. 4*a*, cf. also the modal visualisation in [1]. In fig. 8*c* and *d*, the Strouhal-number region $St = 0.1$ to 1 represents spanwise-periodic structures, similar to the one shown in fig. 7*a* and *b*, albeit the obvious effect of the sweep angle. The modal structures in the region around the peak at $St = 0.06$ feature two-dimensional dynamics, which is in excellent agreement with the two-dimensional aerofoil [2] and infinite straight wing [1]. In the optimal forcing mode, a distinct oblique line impinges at the core of the shock-wave/boundary-layer interaction where the boundary layer separates (see fig. 7*c* and also fig. 8*c*), which is similar to the adjoint mode presented in a previous aerofoil study [2], where a detailed explanation is provided. In essence, Sartor et al. [2] explained this behaviour by the theory of characteristics, pointing towards the fundamental importance

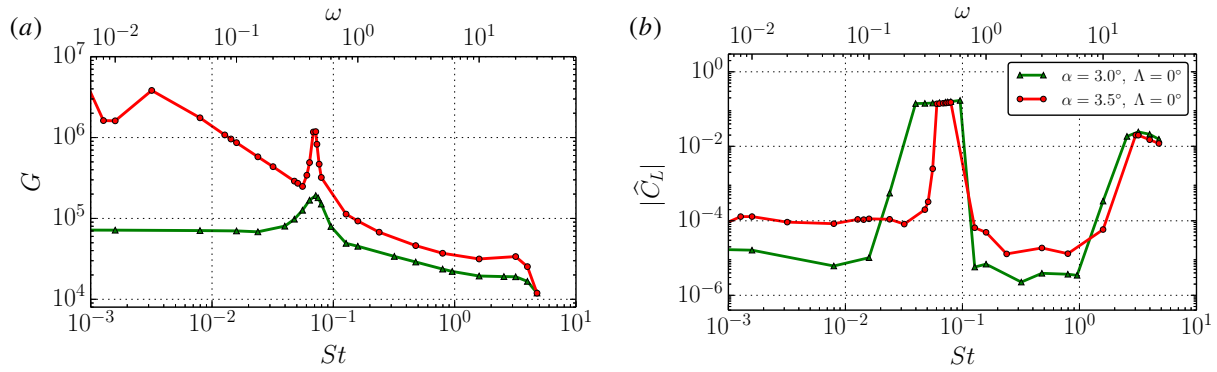

Fig. 5 Straight-wing results showing (a) optimal gain G and (b) magnitude of lift coefficient $|\widehat{C}_L|$.

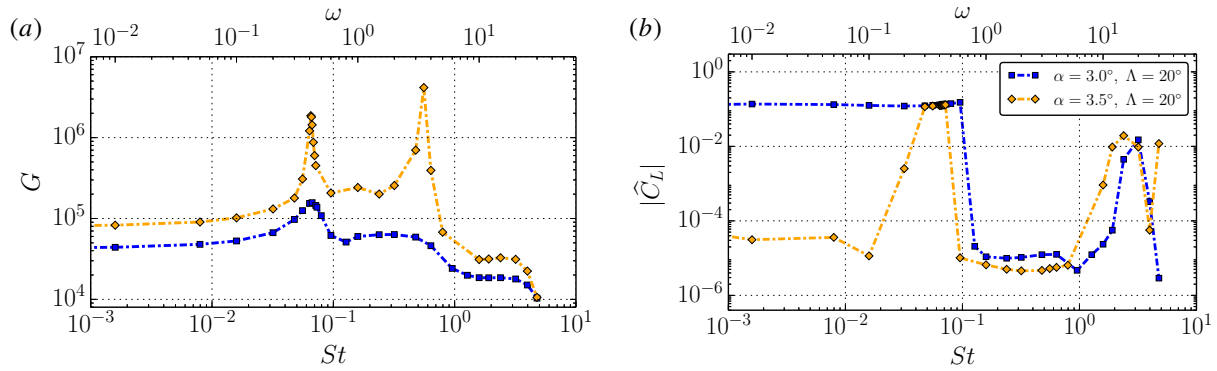

Fig. 6 Swept-wing results showing (a) optimal gain G and (b) magnitude of lift coefficient $|\widehat{C}_L|$.

of the shock foot on the boundary layer separation, and the whole flow field in general, and the travel of information in supersonic flow along characteristic lines. For the third region, forcing and response modes are shown in figs. 7e and f and 8e and f. The modal structures are reminiscent of a Kelvin–Helmholtz shear-layer instability downstream of the shock-wave/boundary-layer interaction. The important message here is that clear modal structures can be identified even in subcritical flow, and such information can hence be used as a predictive method of imminent instability.

Finally, integrating the unsteady pressures gives the lift coefficient, the magnitude of which is shown in figs. 5b and 6b. In principle, its distribution agrees with the discussion on the optimal gain, albeit featuring two rather than three distinct peaks. These peaks result from the spatial distribution of the surface pressure, inferred also from the total energy fluctuations. A strong lift response requires a strong chordwise pressure variation with an overall low spanwise variation, as observed for the modes describing the aerofoil shock-buffet and Kelvin–Helmholtz behaviour. The spanwise-periodic modes, on the other hand, seem to cancel out the pressure fluctuation resulting in low lift variation overall.

D. Mean Flow Approach

The resolvent analysis in the previous section starts from a steady-state RANS solution, called *base flow*. When it is difficult to obtain such a base flow, especially at high Reynolds numbers, *mean flow* could be an alternative option, as reviewed by Mettot et al. [18]. In the current work, a mean flow on the straight wing is obtained by running a time-marching unsteady RANS simulation at angle of attack $\alpha = 3.5°$. The chosen non-dimensional time-step size is $\Delta t = 0.0001$ with 50 to 200 subiterations per physical time-step, and the unsteady run is initialised with a well-converged RANS solution at a density-residual norm of 10^{-12}. The flow grows exponentially until approximately $t = 0.4$, when non-linear saturation starts to dominate, and enters into a stable limit-circle oscillation at $t \approx 0.8$ (see fig. 9a). The mean-flow calculation is started at $t = 1$ for about 8 cycles. The pressure coefficient of the mean flow gives similar result to the base flow, as expected for such a benign angle of attack (see fig. 9b). The shock wave appears slightly smeared indicating a shock motion of about 10% chord extent. Comparison of the subsequent resolvent analyses is presented in

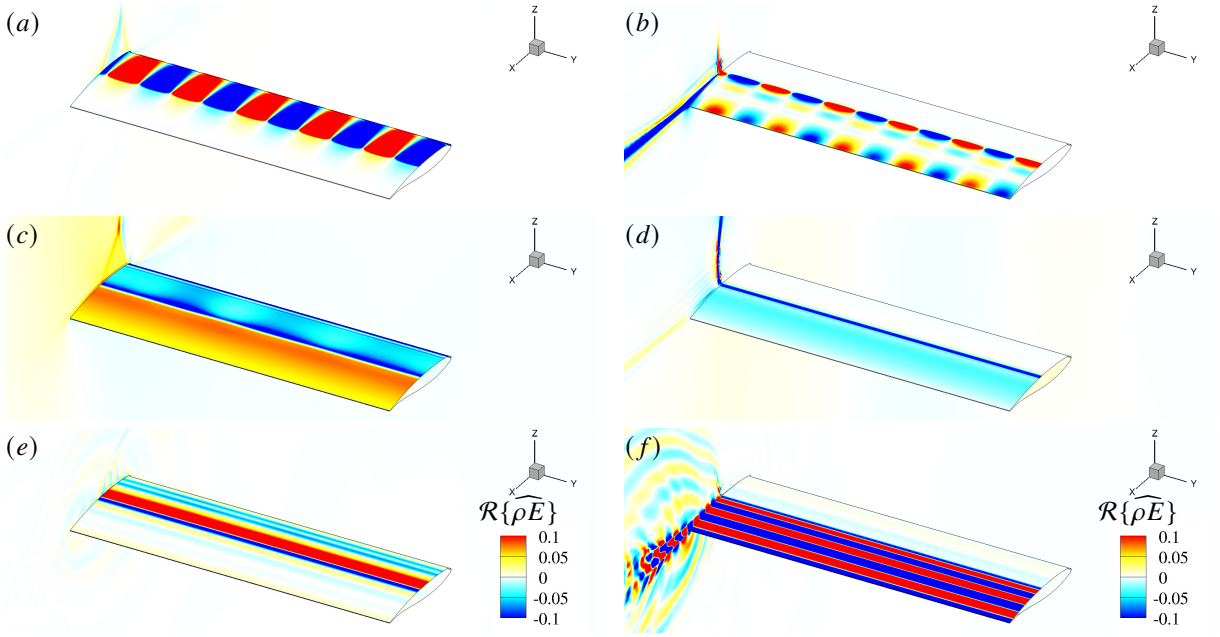

Fig. 7 Real part $\mathcal{R}\{\widehat{\rho E}\}$ of unit-length optimal (a, c, e) forcing and (b, d, f) response modes at $St \approx 0.001$ (top), 0.06 (middle) and 2.75 (bottom) on straight wing at $\alpha = 3.5°$.

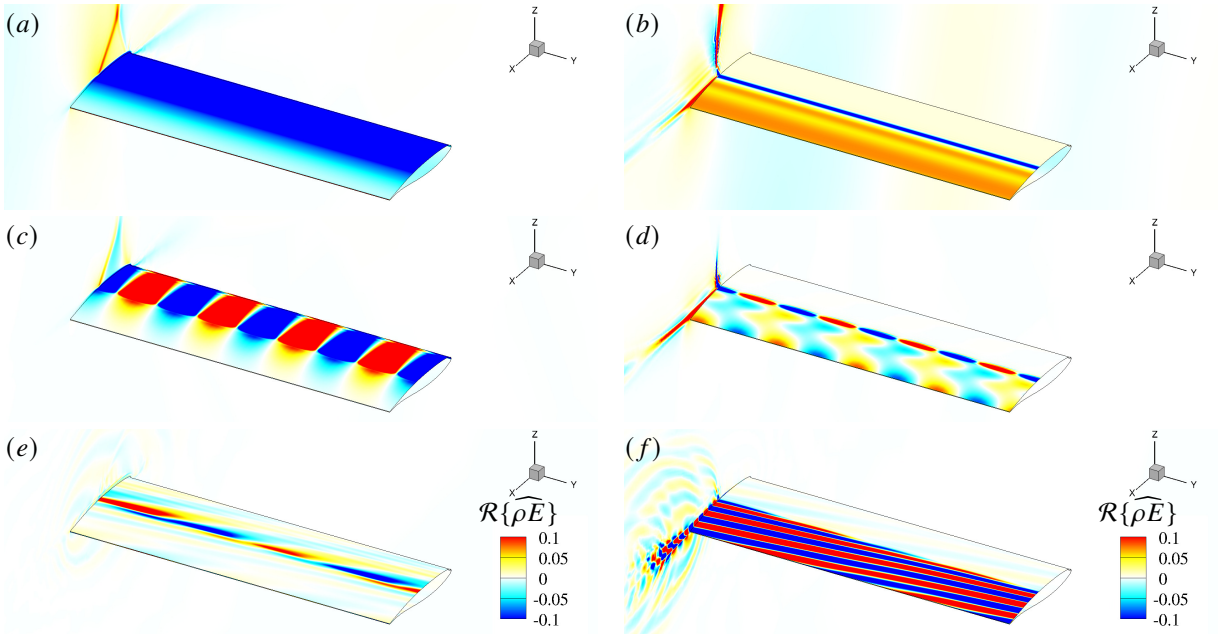

Fig. 8 Real part $\mathcal{R}\{\widehat{\rho E}\}$ of unit-length optimal (a, c, e) forcing and (b, d, f) response modes at $St \approx 0.06$ (top), 0.29 (middle) and 3.66 (bottom) on swept wing at $\alpha = 3.0°$.

fig. 10. It is shown that the mean-flow approach still predicts the underlying features corresponding to the aerofoil mode and shear-layer instability. In contrast, in the low-frequency region for $St < 0.03$, the optimal gain is flatter and an order of magnitude lower than that computed from the base flow. Figure 11 shows a three-cell spanwise-periodic resolvent mode for the mean flow at $St \approx 0.001$, much like the most amplified $1c$-wavelength mode presented in [1]. The resolvent results suggest that these spanwise-periodic monotone modes discovered in the base flow are much less amplified in the

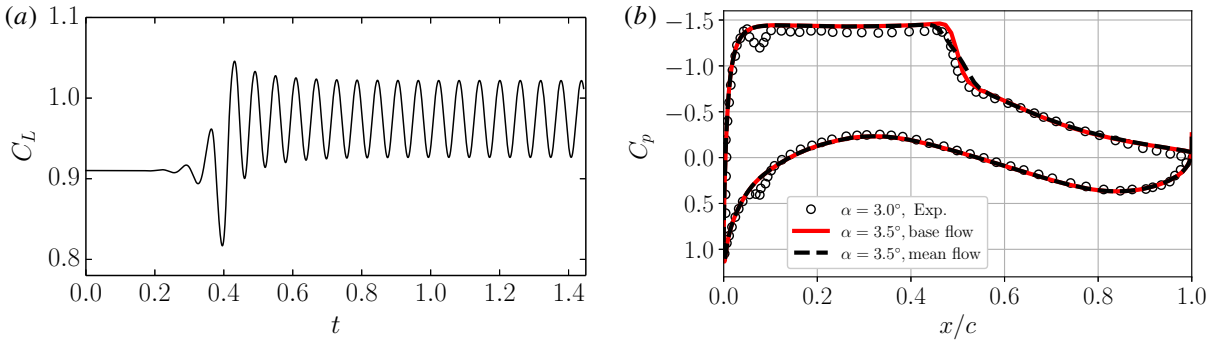

Fig. 9 Straight-wing mean-flow results showing (a) history of lift coefficient and (b) pressure coefficient.

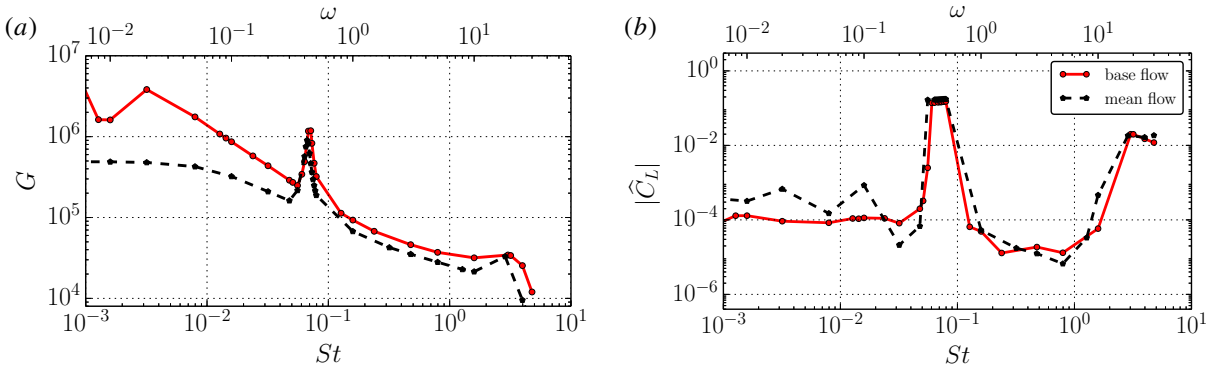

Fig. 10 Comparison of resolvent analysis using both base-flow and mean-flow approach, showing (a) optimal gain G and (b) magnitude of lift coefficient$|\widehat{C}_L|$ on straight wing at $\alpha = 3.5°$.

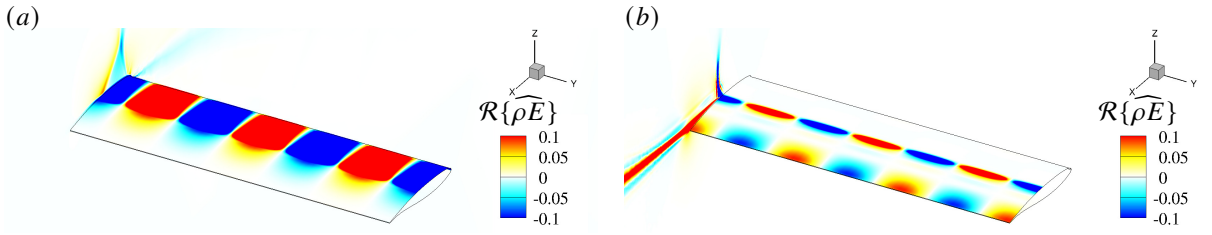

Fig. 11 Real part $\mathcal{R}\{\widehat{\rho E}\}$ of unit-length optimal (a) forcing and (b) response mode for the mean-flow with $St \approx 0.001$ on straight wing at $\alpha = 3.5°$.

mean flow, but this observation requires further scrutiny. Concerning the lift response, there is no significant difference between the two approaches, due to the aforementioned spatial distribution of the unsteady pressure.

V. Conclusions

Three-dimensional resolvent analysis on infinite straight and swept wings at a Mach number of 0.73 and a chord Reynolds number of 3.2×10^6 near the onset of self-sustained transonic unsteadiness, referred to as shock buffet, is discussed. The focus for the swept wing is a 20° sweep angle. Infinite wings are modelled by extruding the OAT15A aerofoil to a given aspect ratio and imposing a spanwise periodic boundary condition. The base flow is a solution to the steady Reynolds-averaged Navier–Stokes equations coupled with the Spalart–Allmaras turbulence model. An inner-outer iterative algorithm is adopted to solve the resolvent problem for the optimal forcing/response modes at a given frequency. We identify three distinct modal features in the transonic flow near shock-buffet onset, and the results

suggest that resolvent analysis can be used to identify an imminent aerodynamic instability even before dominant modes can be clearly identified with global stability tools.

The two-dimensional aerofoil shock-buffet mode, previously reported in the literature, featuring a Strouhal number of $St \approx 0.06$ can be identified both in the straight and swept wing flow. The associated distinct amplification of the optimal gain even in subcritical, globally stable flow is caused both by an emerging eigenvalue and the inherent non-normality of the governing equations, the individual contribution of which needs to be quantified further. The spanwise-periodic monotone modes corresponding to a low Strouhal number ($St < 0.03$) give a high amplification in the supercritical shock-buffet flow on the straight wing, but at the same time this region is less dominant in the subcritical flow. For the swept wing, the highly amplified spanwise-periodic modes shift to higher Strouhal numbers of $St \approx 0.1$ to 1. These results are in good agreement with findings in recent global stability work. Additionally, a mode describing a Kelvin–Helmholtz-type shear-layer instability is found for Strouhal numbers of $St \approx 1$ to 5. In general, the resolvent modes in subcritical flow have a similar topology compared to the post-onset shock-buffet flow. A preliminary resolvent analysis on the straight wing using mean flow reveals that the same aerofoil and Kelvin–Helmholtz modes can be identified. In contrast, a change in behaviour is observed concerning the spanwise-periodic, monotone modes.

In the next step, richer routine data analysis of the current results is required in general, and application of the resolvent analysis to a practical test case would be useful to demonstrate the tool capability.

Acknowledgments

We gratefully acknowledge financial support from the Engineering and Physical Sciences Research Council (grant number EP/R037027/1). We also thank the University of Liverpool and the ARCHER UK National Supercomputing Service (http://archer.ac.uk) for computing time.

References

[1] He, W., and Timme, S., "Triglobal Schock Buffet Instability Study on Infinite Wings," *AIAA Scitech 2020 Forum*, AIAA Paper 2020–1986, Orlando, FL, 2020. https://doi.org/10.2514/6.2020-1986.

[2] Sartor, F., Mettot, C., and Sipp, D., "Stability, Receptivity, and Sensitivity Analyses of Buffeting Transonic Flow over a Profile," *AIAA Journal*, Vol. 53, No. 7, 2015, pp. 1980–1993. https://doi.org/10.2514/1.J053588.

[3] Gómez, F., Sharma, A. S., and Blackburn, H. M., "Estimation of Unsteady Aerodynamic Forces Using Pointwise Velocity Data," *Journal of Fluid Mechanics*, Vol. 804, 2016, p. R4. https://doi.org/10.1017/jfm.2016.546.

[4] Jacquin, L., Molton, P., Deek, S., Maury, B., and Soulevant, D., "Experimental Study of Schock Oscillation over a Transonic Supercritical Profile," *AIAA Journal*, Vol. 47, No. 9, 2009, pp. 1985–1994. https://doi.org/10.2514/1.90190.

[5] He, W., Gioria, R. S., Pérez, J. M., and Theofilis, V., "Linear Instability of Low Reynolds Number Massively Separated Flow around Three NACA Airfoils," *Journal of Fluid Mechanics*, Vol. 811, 2017, pp. 701–741. https://doi.org/10.1017/jfm.2016.778.

[6] Bippes, H., and Turk, M., "Windkanalmessungen in Einem Rechteckflügel bei Anliegender und Abgelöster Strömung," Tech. Rep. IB251-80A18, DFVLR Forschungsbericht, 1980.

[7] Weihs, D., and Katz, J., "Cellular Patterns in Post Stall Flow over Unswept Wings," *AIAA Journal*, Vol. 21, No. 12, 1983, pp. 1757–1759. https://doi.org/10.2514/3.8321.

[8] Yon, S. A., and Katz, J., "Study of the Unsteady Flow Features on a Stalled Wing," *AIAA Journal*, Vol. 36, No. 3, 1998, pp. 305–312. https://doi.org/10.2514/2.372.

[9] Plante, F., Dandois, J., Beneddine, S., Sipp, D., and Laurendeau, E., "Numerical Simulations and Global Stability Analyses of Transonic Buffet and Subsonic Stall," *AAAF AERO2019*, hal–02127307, Paris, France, 2019.

[10] Thiery, M., and Coustols, E., "Numerical Prediction of Shock Induced Oscillations over a 2D Airfoil: Influence of Turbulence Modelling and Test Section Walls," *International Journal of Heat and Fluid Flow*, Vol. 27, 2006, pp. 661–670. https://doi.org/10.1016/j.ijheatfluidflow.2006.02.013.

[11] Garbaruk, A., Shur, M., Strelets, M., and Spalart, P. R., "Numerical Study of Wind-Tunnel Walls Effects on Transonic Airfoil Flow," *AIAA Journal*, Vol. 41, No. 6, 2003, pp. 1046–1054. https://doi.org/10.2514/2.2071.

[12] Crouch, J. D., Garbaruk, A., and Magidov, D., "Predicting the Onset of Flow Unsteadiness Based on Global Instability," *Journal of Computational Physics*, Vol. 224, No. 2, 2007, pp. 924–940. https://doi.org/10.1016/j.jcp.2006.10.035.

[13] Crouch, J. D., Garbaruk, A., and Strelets, M., "Global instability in the onset of transonic-wing buffet," *Journal of Fluid Mechanics*, Vol. 881, 2019, pp. 3–22. https://doi.org/10.1017/jfm.2019.748.

[14] Timme, S., "Global Instability of Wing Shock-Buffet Onset," *Journal of Fluid Mechanics*, Vol. 885, 2020, p. A37. https://doi.org/10.1017/jfm.2019.1001.

[15] Paladini, E., Beneddine, S., Dandois, J., Sipp, D., and Robinet, J.-C., "Transonic Buffet Instability: From Two-dimensional Airfoils to Three-Dimensional Swept Wings," *Physical Review Fluids*, Vol. 4, 2019, p. 103906. https://doi.org/10.1103/PhysRevFluids.4.103906.

[16] Timme, S., and Thormann, R., "Towards Three-Dimensional Global Stability Analysis of Transonic Shock Buffet," *AIAA Atmospheric Flight Mechanics Conference*, AIAA Paper 2016–3848, Washington, D.C., 2016. https://doi.org/10.2514/6.2016-3848.

[17] Barkley, D., "Linear analysis of the cylinder wake mean flow," *Europhysics Letters (EPL)*, Vol. 75, No. 5, 2006, pp. 750–756. https://doi.org/10.1209/epl/i2006-10168-7.

[18] Mettot, C., Sipp, D., and Bézard, H., "Quasi-Laminar stability and sensitivity Analyses for Turbulent Flows: Prediction of Low-Frequency Unsteadiness and Passive Control," *Physics of Fluids*, Vol. 26, No. 4, 2014, p. 045112. https://doi.org/10.1063/1.4872225.

[19] Jovanović, M. R., and Bamieh, B., "Componentwise Energy Amplification in Channel Flows," *Journal of Fluid Mechanics*, Vol. 534, 2005, p. 145–183. https://doi.org/10.1017/S0022112005004295.

[20] Yeh, C.-A., and Taira, K., "Resolvent-Analysis-Based Design of Airfoil Separation Control," *Journal of Fluid Mechanics*, Vol. 867, 2019, p. 572–610. https://doi.org/10.1017/jfm.2019.163.

[21] Taira, K., Brunton, S., Dawson, S., Rowley, C., Colonius, T., McKeon, B., Schmidt, O., Gordeyev, S., Theofilis, V., and Ukeiley, L., "Modal Analysis of Fluid Flows: An Overview," *AIAA Journal*, Vol. 55, No. 12, 2017, pp. 4013–4041. https://doi.org/10.2514/1.J056060.

[22] Symon, S., Rosenberg, K., Dawson, S. T. M., and McKeon, B. J., "Non-Normality and Classification of Amplification Mechanisms in Stability and Resolvent Analysis," *Physical Review Fluids*, Vol. 3, 2018, p. 053902. https://doi.org/10.1103/PhysRevFluids.3.053902.

[23] Bonne, N., Brion, V., Garnier, E., Bur, R., Molton, P., Sipp, D., and Jacquin, L., "Analysis of the Two-Dimensional Dynamics of a Mach 1.6 Shock Wave/Transitional Boundary Layer interaction Using a RANS Based Resolvent Approach," *Journal of Fluid Mechanics*, Vol. 862, 2019, pp. 1166–1202. https://doi.org/10.1017/jfm.2018.932.

[24] Schwamborn, D., Gerhold, T., and Heinrich, R., "The DLR TAU-Code: Recent Applications in Research and Industry," *European Conference on Computational Fluid Dynamics, ECCOMAS CFD 2006*, TU Delft, The Netherlands, 2006.

[25] Allmaras, S. R., Johnson, F. T., and Spalart, P. R., "Modifications and Clarifications for the Implementation of the Spalart-Allmaras Turbulence Model," *Seventh International Conference on Computational Fluid Dynamics*, ICCFD7–1902, Big Island, Hawaii, 2012.

[26] Sorensen, D., "Implicit Application of Polynomial Filters in a k-Step Arnoldi Method," *SIAM Journal on Matrix Analysis and Applications*, Vol. 13, No. 2, 1992, pp. 357–385.

[27] Maschhoff, K. J., and Sorensen, D. C., "P_ ARPACK: An Efficient Portable Large Scale Eigenvalue Package for Distributed Memory Parallel Architectures," *Lecture Notes in Computer Science*, Vol. 1184, 1996, pp. 478–476.

[28] Lehoucq, R., Sorensen, D., and Yang, C., *ARPACK Users' Guide*, SIAM, 1998.

[29] Spalart, P., "Trends in turbulence treatments," *Fluids 2000 Conference and Exhibit*, AIAA Paper 2000–2306, 2000. https://doi.org/10.2514/6.2000-2306.

[30] Nitzsche, J., "A numerical study on aerodynamic resonance in transonic separated flow," *International Forum on Aeroelasticity and Structural Dynamics, IFASD 2009-126*, 2009.